A Multifrequency Multistage Fingerprinting-based Radiolocation System Based

Murat Ambarkutuk
Mechanical Engineering Department,
Virginia Polytechnic Institute and State University,
Blacksburg, Virginia, USA Email:murata@vt.edu

Tomonari Furukawa
Mechanical Engineering Department,
Virginia Polytechnic Institute and State University,
Blacksburg, Virginia, USA Email: tomonari@vt.edu

Abstract*—This paper presents a multifrequency and multistage indoor robot localization system based on fingerprinting. The proposed system relies on a 900 MHz Long Range Radio (LoRa) along with 2.4 GHz Wireless Fidelity (WiFi) and Bluetooth (BT) networks. By exploiting different propagation characteristics of different Radio Frequency (RF) signal wave within a Gated Recurrent Unit (GRU) framework, Received Signal Strength (RSS) measurements are used for indoor localization purposes. Similar to conventional fingerprinting systems, the system is consisted of two phases: data acquisition and learning (offline), and localization (online). In offline phase, the signal maps for various AP's are constructed via RSS information and path loss exponent is learned by a network consisted of GRU, whereas the online phase contains an information fusion based localization method. *Add some result once get it

I. Introduction

Inverse pyramid:

- P1: Background
  1) Inverse pyramid
  2) Last sentence: introduce the area of the title of your paper as a significant topic
  3) 5 refs (books, review papers, journals, no conf)
- P2-3: Background
  1) Original classification: Support the objectives with each sentence
  2) Appreciate their work, their focus however different
  3) no technical words
  4) 10 refs (journal, conference papers)
- P4: Objectives
  1) 1-3 objectives
  2) the first sentence: this paper presents

The organization of the paper as follows. Section II lays out the fundamentals of the radio wave propagation, while Section III covers the details of the proposed system. Section IV-B demonstrates the validity of the proposed system in different environments. In Section V, the experimentation results will be concluded and future work will be addressed.

II. Radio Wave Propagation in Radiolocation

This section will cover the fundamentals of radio wave propagation with regards to Fingerprinting-based Indoor Radiolocation Systems (FIRL). FIRLs consists of two main phases. The first phase, i.e. offline phase, involves with collecting some form of measurements about the anchor nodes placed in the environment, along with the corresponding positions. Let $m_j^i \in \mathbb{Z}^1$ and $d_j^i \in \mathbb{R}^1$ be the measurement obtained from anchor node i at location j, and the radial distance between location j and anchor node i, respectively. The measurement space $\boldsymbol{m}^i = \{m_j^i | j = 1 \dots n_{loc}\} \in \mathbb{R}^{n_{loc}}$ is often constructed in either frequency domain [refer CSI], or time domain. The measurements are then used to approximate the propagation function $f_d^i : \mathbb{Z}^1 \mapsto \mathbb{R}^1$ of anchor node i.

$$f_d^i(m_j^i) = d_j^i \tag{1}$$

One of the most popular fingerprints are Received Signal Strength (RSS) in FIRLs due to its simplicity in acquiring the fingerprints. The fundamental relationship between transmitted and received signal strengths P_t and $P_r(d)$ between ideal antennas in an empty space with a separation distance d is characterized by Friis' Free Space Equation (FFSE) given below [1].

$$P_r(d) = \frac{P_t G_t G_r \lambda^2}{(4\pi d)^2 L} \tag{2}$$

In Equation (2), G_t, and G_r denote the unitless gains of transmitter and receiver antennas, respectively, whereas λ is the wavelength of the radio wave. Moreover, since the received signal strength is often minuscule level, FFSE is denoted in the decibel scale relative to a milliwatt.

$$\begin{aligned} \widetilde{P}_r(d) = \widetilde{P}_t + 10\log G_t + 10\log G_r + \\ 20\log\lambda - 20\log d - 20\log 4\pi \end{aligned} \tag{3}$$

$\widetilde{P}_r(d)$ and $\widetilde{P}_t$ represent received and transmitted signal strengths decibel scale. However, neither Equation (2) nor Equation (3) holds true for the distance $0 < d < \lambda$. Thus, received signal strength is generally denoted relative to a reference point d_0 with a prior corresponding received signal strength.

$$\widetilde{P}_r(d) = \widetilde{P}_r(d_0) + 20\log\frac{d_0}{d} \tag{4}$$

However well-known, neither FFSE nor its variants are able to model major propagation mechanisms, i.e. reflection, diffraction or scattering occurring along the the propagation path, due to the fact that it can only model Line-of-sight (LOS) propagation. Thus, it is often impractical to utilize it in indoor localization problems where reflection and diffraction occurs along the propagation path. Therefore, the path loss occurring along the propagation path can be derived as the sum of the difference between transmitted and received signal strength and other losses occurring along the propagation path. Equation (5) represents a special Path Loss (PL) model, i.e. Log-distance Path Loss (LDPL) which describes the attenuation relative to a reference point. One of the major advantages of LDPL model over FFSE is that LDPL model can account for obstructions and corresponding wave propagation in the space with varying values of PL exponent n.

$$\overline{PL}(d) = \overline{PL}(d_0) + 10n \log \frac{d}{d_0} \tag{5}$$

$$n = \begin{cases} < 2, & \text{if the space structure guides the radio waves along the propagation path} \\ = 2, & \text{if the space is empty,} \\ > 2, & \text{if there are obstructions along the propagation path} \end{cases} \tag{6}$$

One of the most common solution in FIRLs is to estimate n by fitting a curve to collected fingerprints. Given a mean PL at an unknown location $\overline{PL}(d)$, PL exponent n and a mean PL at the reference point d_0 $\overline{PL}(d_0)$, the propagation function of anchor node i f_d^i can be obtained by solving LDPL for the radial distance d^i.

$$f_d^i = d_0^i 10^{\left(\dfrac{\overline{PL}(d) - \overline{PL}(d_0)}{10n}\right)} = d_j^i \tag{7}$$

However, in order to obtain radial distance from anchor node i d^i, PL exponent n should be estimated from the data collected during the offline phase. Let $\boldsymbol{m}^i = \{\widetilde{P}_r^{i,j}(d) | j = 1 \ldots n_{loc}\}$ and $\boldsymbol{d}^i = \{d_j^i | j = 1 \ldots n_{loc}\}$ be the RSS fingerprints acquired from anchor node i during surveying and corresponding distances from anchor node i, respectively. The estimated radial distance from anchor node i $\hat{d}^i$ can be obtained with an approximated propagation function $\hat{f}_d^i(m_j^i, n_i^*)$.

$$\hat{f}_d^i(m_j^i, n_i^*) = d_0^i 10^{\left(\dfrac{\widetilde{P}_t - \widetilde{P}_r^{i,j}(d) - \overline{PL}(d_0)}{10n_i^*}\right)} = \hat{d}_j^i \tag{8}$$

where n^* is the overall PL exponent which minimizes the sum of the absolute localization error.

$$n_i^* = \arg\min_n \sum_j |d_j^i - f_d^i(m_j^i, n)| \tag{9}$$

After obtaining the approximated propagation function, the measurements acquired from the anchor nodes are mapped to relative radial distances in order to distinguish the absolute position of the agent in the environment, which forms the offline phase of the FIRLs.

III. MULTIFREQUENCY MULTISTAGE RADIOLOCATION SYSTEM

This section explains Multifrequency Multistage Radiolocation System (MFMS) in greater detail. Akin to other FIRLs, MFMS consists of two main phases. During the offline phase, RSS information from anchor nodes is collected at many locations in the environment and used to approximate the radio wave propagation function. The online phase, on the other hand, makes use of the approximated propagation function obtained in the former phase. However, one major difference between MFMS and conventional FIRL approaches is that MFMS employs three types of radio setups in three different stages to infer the location of the agent.

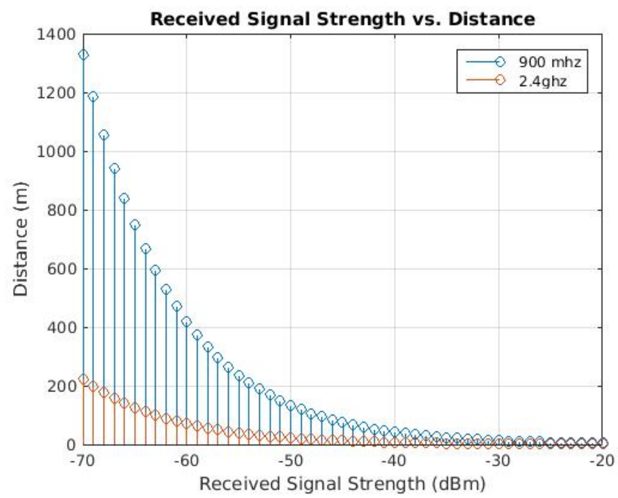

Fig. 2: RSSI readings of NLoS and LoS APs acquired with a stationary agent

The main motivation behind employing multisource information is to exploit the diversity of the propagation characteristics of the different frequencies. As can be seen in the Equation (5) and Figure 2, the received power and separation distance shows a log-linear relationship. This figure implies two fundamental problems in radiolocation systems: The first problem is that as the carrier frequency increases path loss increases significantly, which limits the radio covarage and localization ability of the system in large environments. On the other hand, as the carrier frequency increases, the separation between two antennas, i.e. the anchor node and the target to be localized, can be identified with finer spatial resolution. Therefore, the trade-off between radio coverage and spatial localization resolution can be resolved by employing different frequencies in indoor localization systems by fusing the information acquired from the anchor nodes using different carrier frequencies. Thus, MFMS employs a Long Range Radio (LoRa) (900 MHz), a WiFi Access Point (AP) and a Bluetooth (2.4 GHz) beacon in each anchor node. Table I tabulates the specifications of the radios consisting in each anchor node, while Figure 3 demonstrates the details of the anchor nodes. In detail, wider spatial coverage is achieved by

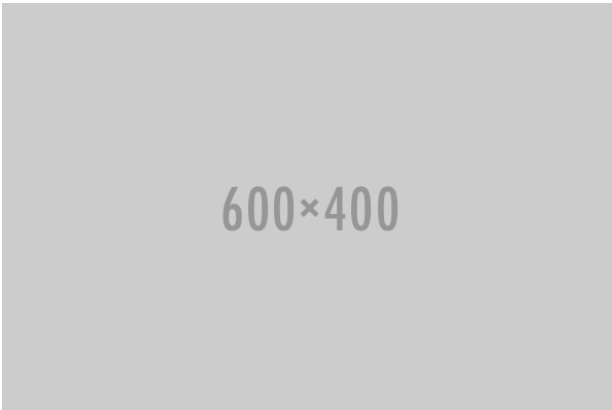

(a) Floor map of the first environment used in the experimentations

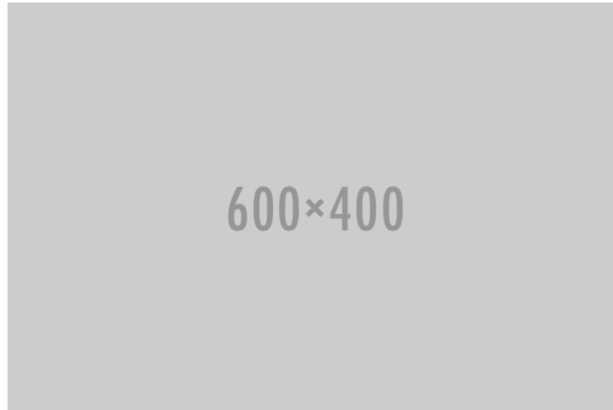

(b) Floor map of the first environment used in the

Fig. 1: The floor maps of the environments was conducted

TABLE I: The specifications of radios used in anchor nodes

Property	WiFi	Bluetooth	LoRa
Frequency [MHz]:	2400	2400	900
Communication Bandwidth:	1-11 Mbps	Upto 4 Mbps	10 Kbps
Transmission Power P_t [dBm]:	17	10	24
Reciever Sensivity [dBm]:	?	-98	-101
Communication Range [m]:	$<$20	10	$>$100

using LoRa modules working at 900 MHz while finer spatial resolution provided by WiFi and Bluetooth both working at 2.4 GHz frequency.

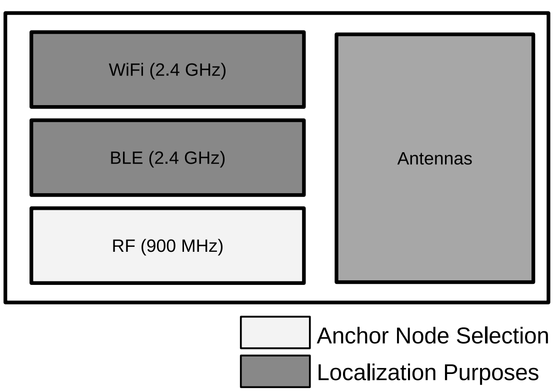

Fig. 3: MFMS Anchor Nodes

A. Spatially-coherent Path Loss Exponent Estimation

This section covers the details of the joint path loss exponent estimation which forms the first stage of MFMS. We approach the FIRL problem in the scope of curve fitting. However, unlike many approaches proposed mentioned earlier, MFMS does not try to blindly fit a function which best explains the training data given the location labels. Moreover, MFMS does not consider the path loss exponent as a variable describing the whole localization environment. Instead, we approach the problem as curve fitting for path loss exponent differing in value depending on the regions at which the agent resides. In other words, the path loss exponent for MFMS is a function of both location. Therefore, the proposed system is able account for non-uniform distribution of obstructions in space.

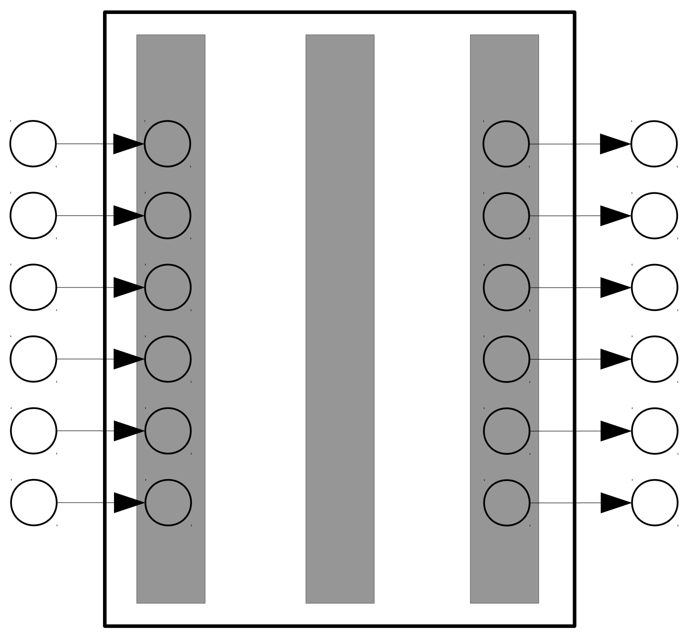

Fig. 4: The softmax classifier assigns weights for each anchor node based on the evidence representing the probability of residing in a grid cell g.

Let $\Omega = \{g_i | i = 1 \dots n_{grid}\}$, is the localization environment which is divided into n_{grid} number of grids g. An arbitrary position $\boldsymbol{x} \in \Omega$ can be in a shadowed region for any anchor node; thus, MFMS selectively chooses which anchor nodes to use to localize the agent in Ω. This selection is performed by mapping the measurement vector acquired at time step k $\boldsymbol{m}_j^k \in \mathbb{Z}^{n_{node}}$ with a set of weights $\boldsymbol{w}_g \in \mathbb{R}^{n_{node}}$ such that $\sum_g \boldsymbol{w}_g = 1$. The weights of each grid is learned with a softmax classifier, which is depicted in Figure 4. The classifier is solely based on LoRa measurements due to the higher probability of observing multiple LoRa modules in arbitrary positions in the environment, thanks to the smaller path loss they introduce. Equation (10) shows the result of the selection process.

$$\widetilde{\boldsymbol{m}}_j^k = \boldsymbol{w}_g \boldsymbol{m}_j^k \tag{10}$$

For each anchor node, the path loss exponent is estimated with LDPL model in a least square sense. The estimated spatially-coherent path loss exponent, a set physical parameter defining the radio wave propagation, is incorporated into the location estimation process explained in Stage-II.

$$n_g^{*,i} = \underset{n}{\arg\min} \sum_j \Big(\|\boldsymbol{x}_g\|_2 - f_d(m_{j_g}^i, n) \Big)^2 \tag{11}$$

where $\boldsymbol{x}_g$ and $m_{j_g}^i$ denote the center position of grid g, and measurements acquired in grid g, while $f_d(\cdot)$ denotes LDPL model.

B. Pinpoint Localization

This section gives details of the second stage of the MFMS which is the pinpoint localization. After localizing the agent in grid-level and selecting which anchor nodes to be employed, the propagation function $\hat{g}_d(\cdot)$ can be formulated as below:

$$\hat{g}_d(\widetilde{\boldsymbol{m}}_j^{k-n_m:k}, \boldsymbol{n}_g^*) = \hat{\boldsymbol{x}} \tag{12}$$

where $\widetilde{\boldsymbol{m}}_j^{k-n_m:k}$, $\boldsymbol{n}_g^*$, and $\hat{\boldsymbol{x}}$ are the weighted measurement vector between time steps $k - n_m$ and k, the estimated path loss exponent vector of each anchor node for grid g and the estimated absolute position of the agent, respectively. As can be seen in Equation (12), the propagation function incorporates the weighted measurements with the spatially- and temporally-coherent path loss exponent so that the physical characteristics of the radio waves, represented with the path loss, are enforced into the model as a parameter.

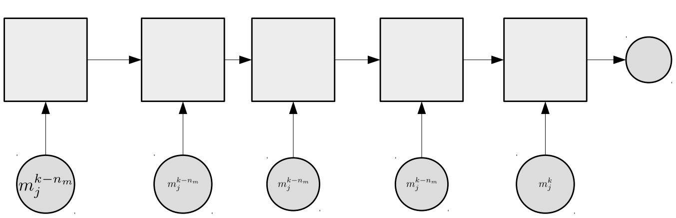

Fig. 5: GRU

The propagation function of WiFi $\hat{g}_d^w(\cdot)$ and Bluetooth $\hat{g}_d^b(\cdot)$ anchors are approximated with two separate recurrent neural networks, consisting of three layers of Gated Recurrent Unit (GRU) [2]. These functions are attained with a Stochastic Gradient Descent (SGD) based back-propagation algorithm. After approximating the propagation functions, these are employed to estimate the location of the agent. Specifically, the pinpointing algorithm incorporates the spatially-coherent path loss exponent along with the weighted measurements to estimate $\hat{\boldsymbol{x}}^w$ and $\hat{\boldsymbol{x}}^b$, estimated positions by using WiFi measurements and Bluetooth measurements, respectively.

Figure 5 depicts the Stage-II of MFMS in an unfolded representation.

C. Information Fusion

This section of the paper further explains the Stage-III of the MFMS. The Stage-III is essentially an information fusion layer of the model where location estimates of WiFi and Bluetooth measurements are fused into one final entity. The incorporation of two estimates are achieved in the framework of a Neural Network (NN) consisting of 3 layers. The network is in a gradually narrowing structure such that the first, second and last layer contain 8, 4, 2 neurons, respectively. Figure 6 demonstrates the Phase-III.

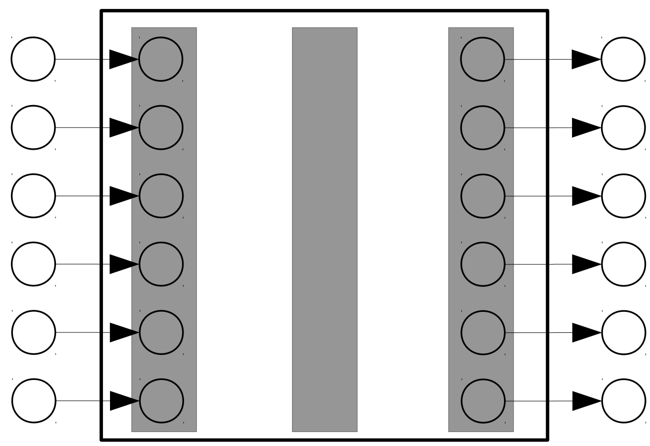

Fig. 6: Two location estimates of WiFi and Bluetooth approximations are fused with a 3 layered-NN.

IV. Experimentation

A. Experimental Setup

This section will lay out the outline of the experimantation conducted. The experimentations are conducted on two different environments depicted on Figure 1. The first environment is a such-by-so area with no obstructions, while the second environment resides in a basement of Randolph Hall, Virginia Tech. The second environment consists of narrow corridors which results in multipath propagation due to reflection and guiding effect of the walls. The circles on Figure 1 denote the location of the anchor nodes, while the grid size is set to be 50 centimeters, approximately 4 times of the wavelength of the WiFi and Bluetooth. Therefore, environment 1 and environment 2 consists of such and so grids, respectively. The efficacy of different stages of MFMS is investigated separately and all-combined. The first experimentation investigates the accuracy of grid-level localization which forms the Stage-I is examined in a statistical manner, while second experimentation investigates the accuracy of pinpoint localization stage. Later, the efficacy of the information fusion stage is investigated by comparing the results of individual WiFi and Bluetooth estimates to the fused estimates. The validity of MFMS is studied by repeating the experiments on two different environments of different sizes which introduces different level of obstructions.

1) Hardware: The anchor nodes used during the experimentations depicted on Figure 3. In detail, MFMS employes low-cost and off-the-shelf radio modules in the design of the anchor nodes. Each anchor node contains an XBee, referred as LoRa working at 900 MHz, and a ESP32 containing a WiFi access point and a Bluetooth working at 2.4 GHz. Table I lays out the details of the individual module specification in detail. The mobile agent is equipped with an ESP32 and a low-cost Bluetooth module based on CSR8510 chipset.

2) Software: LoRa, WiFi, and Bluetooth measurements are collected with the module placed on the mobile agent, and transmitted to onboard computer via Serial communication protocol. The synchronization of the radios along with the parsing of the serial packets are implemented with ROS [3]. The approximation of the propagation function is achieved with the help of Keras [4] which uses Tensorflow [5] as the backend.

B. Results

Lorem ipsum dolor sit amet, consectetur adipisicing elit, sed do eiusmod tempor incididunt ut labore et dolore magna aliqua. Ut enim ad minim veniam, quis nostrud exercitation ullamco laboris nisi ut aliquip ex ea commodo consequat. Duis aute irure dolor in reprehenderit in voluptate velit esse cillum dolore eu fugiat nulla pariatur. Excepteur sint occaecat cupidatat non proident, sunt in culpa qui officia deserunt mollit anim id est laborum.

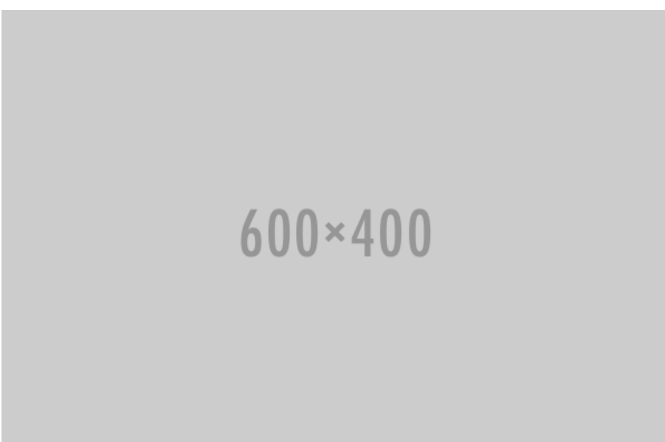

Fig. 7: The confusion matrix obtained during grid-selection.

Lorem ipsum dolor sit amet, consectetur adipisicing elit, sed do eiusmod tempor incididunt ut labore et dolore magna aliqua. Ut enim ad minim veniam, quis nostrud exercitation ullamco laboris nisi ut aliquip ex ea commodo consequat. Duis aute irure dolor in reprehenderit in voluptate velit esse cillum dolore eu fugiat nulla pariatur. Excepteur sint occaecat cupidatat non proident, sunt in culpa qui officia deserunt mollit anim id est laborum. Lorem ipsum dolor sit amet, consectetur adipisicing elit, sed do eiusmod tempor incididunt ut labore et dolore magna aliqua. Ut enim ad minim veniam, quis nostrud exercitation ullamco laboris nisi ut aliquip ex ea commodo consequat. Duis aute irure dolor in reprehenderit in voluptate velit esse cillum dolore eu fugiat nulla pariatur. Excepteur sint occaecat cupidatat non proident, sunt in culpa qui officia deserunt mollit anim id est laborum.

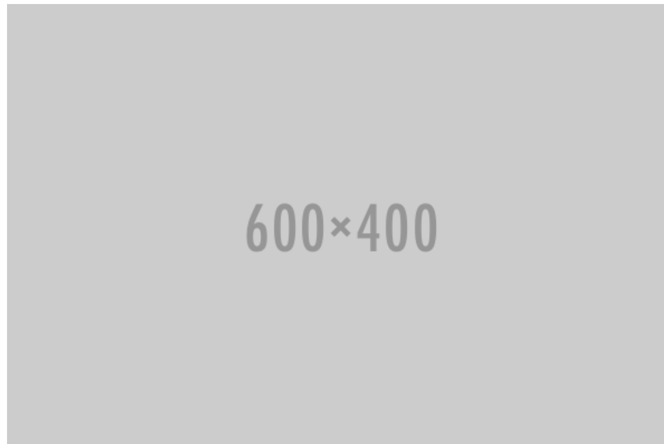

Fig. 8: Cumulative Distribution Function of the Localization Error in both environment: The red, blue and green lines depict localization error occurred when WiFi, Bluetooth and fused measurements are used in localization, respectively.

Lorem ipsum dolor sit amet, consectetur adipisicing elit, sed do eiusmod tempor incididunt ut labore et dolore magna aliqua. Ut enim ad minim veniam, quis nostrud exercitation ullamco laboris nisi ut aliquip ex ea commodo consequat. Duis aute irure dolor in reprehenderit in voluptate velit esse cillum dolore eu fugiat nulla pariatur. Excepteur sint occaecat cupidatat non proident, sunt in culpa qui officia deserunt mollit anim id est laborum. Lorem ipsum dolor sit amet, consectetur adipisicing elit, sed do eiusmod tempor incididunt ut labore et dolore magna aliqua. Ut enim ad minim veniam, quis nostrud exercitation ullamco laboris nisi ut aliquip ex ea commodo consequat. Duis aute irure dolor in reprehenderit in voluptate velit esse cillum dolore eu fugiat nulla pariatur. Excepteur sint occaecat cupidatat non proident, sunt in culpa qui officia deserunt mollit anim id est laborum.

V. Conclusions and Future Work

1) P-1: Summary: Copy and paste from “this paper presents”, paraphrase it, while summarizing it.
2) P-2: Results and Conclusions: Copy preface of numerical results section. For each results, add a resulting remark. Then conclude with a statement: “Results have demonstrated the effectiveness and applicability of the proposed approach.”
3) P-3: Future work: This paper has focused on . . . and much work is still left open; describe a few future works.

Lorem ipsum dolor sit amet, consectetur adipisicing elit, sed do eiusmod tempor incididunt ut labore et dolore magna

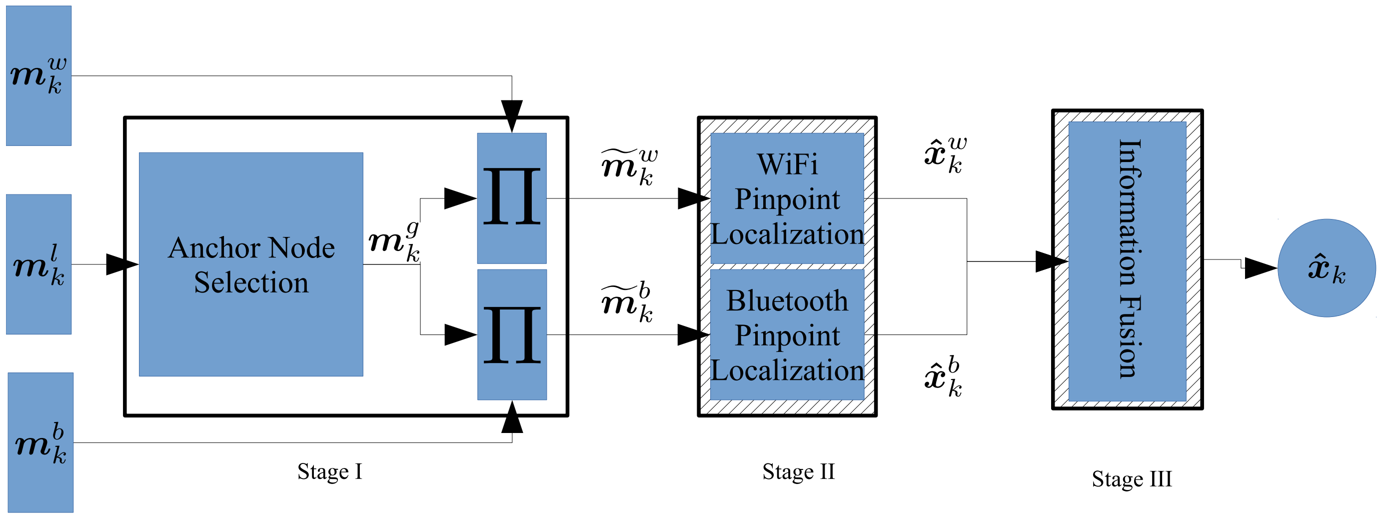

Fig. 9: MFMS Model

aliqua. Ut enim ad minim veniam, quis nostrud exercitation ullamco laboris nisi ut aliquip ex ea commodo consequat. Duis aute irure dolor in reprehenderit in voluptate velit esse cillum dolore eu fugiat nulla pariatur. Excepteur sint occaecat cupidatat non proident, sunt in culpa qui officia deserunt mollit anim id est laborum. Lorem ipsum dolor sit amet, consectetur adipisicing elit, sed do eiusmod tempor incididunt ut labore et dolore magna aliqua. Ut enim ad minim veniam, quis nostrud exercitation ullamco laboris nisi ut aliquip ex ea commodo consequat. Duis aute irure dolor in reprehenderit in voluptate velit esse cillum dolore eu fugiat nulla pariatur. Excepteur sint occaecat cupidatat non proident, sunt in culpa qui officia deserunt mollit anim id est laborum.

Lorem ipsum dolor sit amet, consectetur adipisicing elit, sed do eiusmod tempor incididunt ut labore et dolore magna aliqua. Ut enim ad minim veniam, quis nostrud exercitation ullamco laboris nisi ut aliquip ex ea commodo consequat. Duis aute irure dolor in reprehenderit in voluptate velit esse cillum dolore eu fugiat nulla pariatur. Excepteur sint occaecat cupidatat non proident, sunt in culpa qui officia deserunt mollit anim id est laborum. Lorem ipsum dolor sit amet, consectetur adipisicing elit, sed do eiusmod tempor incididunt ut labore et dolore magna aliqua. Ut enim ad minim veniam, quis nostrud exercitation ullamco laboris nisi ut aliquip ex ea commodo consequat. Duis aute irure dolor in reprehenderit in voluptate velit esse cillum dolore eu fugiat nulla pariatur. Excepteur sint occaecat cupidatat non proident, sunt in culpa qui officia deserunt mollit anim id est laborum.

Lorem ipsum dolor sit amet, consectetur adipisicing elit, sed do eiusmod tempor incididunt ut labore et dolore magna aliqua. Ut enim ad minim veniam, quis nostrud exercitation ullamco laboris nisi ut aliquip ex ea commodo consequat. Duis aute irure dolor in reprehenderit in voluptate velit esse cillum dolore eu fugiat nulla pariatur. Excepteur sint occaecat cupidatat non proident, sunt in culpa qui officia deserunt mollit anim id est laborum. Lorem ipsum dolor sit amet, consectetur adipisicing elit, sed do eiusmod tempor incididunt ut labore et dolore magna aliqua. Ut enim ad minim veniam, quis nostrud exercitation ullamco laboris nisi ut aliquip ex ea commodo consequat. Duis aute irure dolor in reprehenderit in voluptate velit esse cillum dolore eu fugiat nulla pariatur. Excepteur sint occaecat cupidatat non proident, sunt in culpa qui officia deserunt mollit anim id est laborum.

Acknowledgments

References

[1] H. T. Friis, "A note on a simple transmission formula," *Proceedings of the IRE*, vol. 34, no. 5, pp. 254–256, 1946.
[2] K. Cho, B. Van Merriënboer, C. Gulcehre, D. Bahdanau, F. Bougares, H. Schwenk, and Y. Bengio, "Learning phrase representations using rnn encoder-decoder for statistical machine translation," *arXiv preprint arXiv:1406.1078*, 2014.
[3] M. Quigley, K. Conley, B. Gerkey, J. Faust, T. Foote, J. Leibs, R. Wheeler, and A. Y. Ng, "Ros: an open-source robot operating system," in *ICRA workshop on open source software*, vol. 3, no. 3.2. Kobe, Japan, 2009, p. 5.
[4] F. Chollet, "keras," https://github.com/fchollet/keras, 2015.
[5] M. Abadi, A. Agarwal, P. Barham, E. Brevdo, Z. Chen, C. Citro, G. S. Corrado, A. Davis, J. Dean, M. Devin, S. Ghemawat, I. Goodfellow, A. Harp, G. Irving, M. Isard, Y. Jia, R. Jozefowicz, L. Kaiser, M. Kudlur, J. Levenberg, D. Mané, R. Monga, S. Moore, D. Murray, C. Olah, M. Schuster, J. Shlens, B. Steiner, I. Sutskever, K. Talwar, P. Tucker, V. Vanhoucke, V. Vasudevan, F. Viégas, O. Vinyals, P. Warden, M. Wattenberg, M. Wicke, Y. Yu, and X. Zheng, "TensorFlow: Large-scale machine learning on heterogeneous systems," 2015, software available from tensorflow.org. [Online]. Available: http://tensorflow.org/